ISSN 1990-7931, Russian Journal of Physical Chemistry B, 2022, Vol. 16, No. 3, pp. 399–406. © Pleiades Publishing, Ltd., 2022.
Russian Text © The Author(s), 2022, published in Khimicheskaya Fizika, 2022, Vol. 41, No. 6, pp. 7–14.

KINETICS AND MECHANISM OF CHEMICAL REACTIONS, CATALYSIS

Oxidative Cracking of Propane in a Plug-Flow Laboratory Reactor

A. S. Palankoeva[a, b, *], A. A. Belyaev[a], and V. S. Arutyunov[a, b, c]

[a] *Semenov Federal Research Center of Chemical Physics, Russian Academy of Sciences, Moscow, Russia*
[b] *Moscow State University, Moscow, Russia*
[c] *Institute of Problems of Chemical Physics, Russian Academy of Sciences, Chernogolovka, Russia*
**e-mail: anitadmitruk@gmail.com*

Received December 6, 2021; revised January 17, 2022; accepted January 20, 2022

Abstract—This paper presents the results of experiments on the oxidative cracking of propane at a pressure of 1 to 2 atm and moderate temperatures ($T \leq 1000$ K) in a laboratory-scale reactor. Nitrogen and methane are used as the diluent gases. Kinetic models are analyzed to describe the studied process. The necessity of taking into account heterogeneous reactions on the reactor surface is shown. The introduction of additional stages in the kinetic model, which take into account heterogeneous reactions on the reactor surface, makes it possible to obtain an almost quantitative agreement between the calculations and experimental results.

Keywords: natural gas, propane, oxidative cracking, kinetic modeling, heterogeneous reactions
DOI: 10.1134/S1990793122030204

INTRODUCTION

The growing interest in gas-chemical processes for processing natural gas and its individual components is stimulatng the development of more reliable kinetic models to describe these processes occurring in the moderate temperature region ($T \leq 1000$ K). There are only a few models that more-or-less reliably describe the oxidation of the closest methane homologs (including propane) at moderate temperatures. Many of the models presented in the literature, which contain a block of propane oxidation reactions, were created for experimental conditions that differ significantly from the area studied in this paper. In order to analyze the applicability of the most popular published models for describing the processes of propane oxidation and cracking at moderate temperatures, experimental studies of propane oxidative cracking (oxycracking) in a plug-flow laboratory reactor and their kinetic modeling based on the most modern published mechanisms were carried out.

EXPERIMENTAL

Experiments on the oxidative cracking of propane were carried out in a laboratory plug-flow type quartz reactor in the temperature range 773–1023 K and pressure 1–2 atm. The initial propane/oxygen ratio was in the range of 1 to 3. The length of the reactor was 350 mm and the inner diameter was 14 mm. The ratio of the area of the inner surface of the reactor to its volume in the working part, taking into account the surface of the pockets for thermocouples, was 5.4 cm^{-1}. The residence time of the gas mixture in the reactor was constant (2.02 ± 0.05 s). The reactor was heated by three independent electric heaters, which made it possible to maintain a constant temperature profile in the high-temperature zone of the reactor, which was 200 mm long. The laboratory setup used is described in more detail in [1–5], which are continued in this study.

The following gases were used in the experiments: oxygen of high purity (99.7%), high purity nitrogen of the first grade (99.999%), helium grade A (99.995%), and pure propane (99.99%). Nitrogen and methane were used as the gas medium. The gas mixtures at the inlet and outlet of the reactor were analyzed using a Kristall 5000 gas chromatograph manufactured by Khromatek (Russia) equipped with three detectors: one flame ionization detector (FID) and two thermal conductivity detectors (TCDs). In TCD *1*, the presence of H_2 (carrier gas, argon) was determined; in TCD *2*, the presence of CO_2, O_2, N_2, and CO (carrier gas, helium); and in the FID, the presence of hydrocarbons (carrier gas, helium).

KINETIC SIMULATION OF PROPANE OXIDATIVE CRACKING

For modeling, several kinetic models were selected that could be considered to describe the propane oxycracking process in the moderate temperature range: UBC Mech 2.0 kinetic mechanism (UBC) [6], methane/propane oxidation mechanism (methane/propane) [7], C_1–C_3 San Diego Mechanism (San Diego) [8], C_1–C_5 alkane oxidation mechanism (C_1–C_5) [9],

Table 1. Kinetic models of propane oxidation

Mechanism	Number of stages/particles	Applicability conditions	Note
UBC	55/278	R = 15.79–39.48 atm T = 900–1600 K	Based on the GRI-Mech mechanism, supplemented By reactions related to the formation of methylperoxy, ethylperoxy, and propylperoxy radicals
Methane/Propane	38/190	R = 5.3–31.4 atm T = 1042–1585 K	The importance of $CH_3O^{\bullet}$, $CH_3O_2^{\bullet}$ and $CH_3^{\bullet}$ + $O_2/HO_2^{\bullet}$ reactions when describing the kinetics of the process
San Diego	40/235	R = 0.5–50 atm T = 500–2500 K	Included reaction block for C_4
C_1–C_5	293/1588	R = 7.9–29.61 atm T = 630–1550 K	
BUTAN NUI	289/1580	R = 1–30 atm T = 630–1598 K	
HEXANE NUI	913/4150	P = 1–29.61 atm T = 530–1365 K	Based on the AramcoMech 1.3 mechanism [22]. Alternative isomerization reactions of peroxylalkyl hydroperoxide radicals are considered, leading to a More detailed description of this type of intermediate product
HEPTANE NUI	1268/5336	T = 500–1412 K R = 1–37 atm	Submechanism C_0–C_4 from AramcoMech 2.0 [23, 24]
NG HIGH	137/821	R = 1–30 atm T = 1050–1600 K	Radicals i-$C_4H_9O_2$ and their subsequent low-temperature reactions are not included in the model
NG LOW	289/1580	R = 1–30 atm T = 720–1050 K	
NG3	230/1328	P = 1–30 atm T = 630–1598 K	Based on NG, NG HIGH and NG LOW
Ranzi	250/8000	R = 1–20 atm T = 300–2200 K	Includes blocks: C_1–C_4, reference fuel alkanes (n-heptane, isooctane, n-decane, n-dodecane), cycloalkanes (cyclohexane and methylcyclohexane) and aromatic hydrocarbons (benzene, toluene, xylene and ethylbenzene); oxygenated fuels from alcohols, C_3H_6O isomers, ethers (dimethyl ether and ethyl tert-butyl ether), and methyl ethers up to methyl decanoate
NUIGMech	2746/11270	P = 1–40 atm T = 689–2615 K	Based on AramcoMech 3.0 [25]

Butan NUIGALWAY (Butan NUI) [10–14], HEXANE NUIGALWAY (HEXANE NUI) [15], HEPTANE NUIGALWAY (HEPTANE NUI) [16], natural gas to/including C_5 (2007/08) HIGH (NG HIGH), natural gas to/including C_5 (2007/08) LOW (NG LOW), natural gas (NG) [17], natural gas to/including C_5 (2010) (NG3) [5–9], C_1–C_{16} HT + LT + NO_x mechanism (Ranzi) [18], and NUIGMech 1.1. (NUIGMech) [19, 20]. It should be noted that we did not use the well-known mechanism GRI-Mech 3.0 [21] for modeling due to the strong differences between the experimental conditions on which its

Table 2. Heterogeneous reactions involved in the propane oxidation mechanism

Reaction	A, s^{-1}	B	E, cal/mol
$HO_2 \rightarrow HO_{2s}$	2.97×10^{-2}	1.13	509.0
$H_2O_2 \rightarrow H_2O_{2s}$	3.76×10^{-1}	0.50	320.0
$CO \rightarrow CO_s$	2.49×10^{-4}	0.50	0.0

development was based and the conditions considered in this paper. Table 1 gives brief characteristics of the considered mechanisms.

All the mechanisms presented above were developed to describe the processes of light hydrocarbon oxidation and, as a result, they include a propane oxidation block. The mechanisms of the AramcoMech series were not considered, since they are based on other mechanisms that are discussed in detail in this article.

Kinetic modeling was carried out using models of the oxidation of light hydrocarbons in the region of moderate temperatures indicated in Table 1. These models were selected from those presented in the literature according to the criterion of the presence of block C_3 in them and the similarity of the conditions of the experiments in which these models were validated with the conditions of this study. It should be noted that all the considered models were developed exclusively for gas-phase processes and they do not take into account the reactions on the reactor surface, the importance of which was shown by us in [26].

According to [27], the oxycracking of light alkanes proceeds by a chain mechanism with degenerate chain branching as a result of the formation of hydrogen peroxide H_2O_2, formed as a result of the interaction of the peroxide radical $HO_2^{\bullet}$ with an alkane, followed by the decomposition of hydrogen peroxide into $OH^{\bullet}$ hydroxyl radicals. The need to take into account heterogeneous processes in the oxycracking of ethane, and hence other light alkanes, was substantiated in [26]. The same methodology was also given there, including the calculation of accommodation coefficients γ_i for the interaction of the corresponding molecules with the quartz surface of the reactor. Therefore, the NUIGMech mechanism, which showed the best descriptive ability in the preliminary analysis, was supplemented by three heterogeneous reactions involving radicals $HO_2^{\bullet}$, as well as H_2O_2 and CO molecules, which ensure the conversion of peroxide radicals and hydrogen peroxide into water and oxygen molecules on the reactor surface, and carbon monoxide into carbon dioxide (Table 2). It was assumed that the H_2O, O_2, and CO_2 products formed as a result of desorption are almost instantaneously returned to the gas phase compared to the characteristic times of the change in the gas-phase concentrations of $HO_2^{\bullet}$, H_2O_2, and CO.

The corresponding rate constants and accommodation coefficients of particles on the surface to describe the experimental results on propane oxycracking in a quartz reactor were calculated according to the procedure described in [26, 28]. The simulation was carried out in the software environment of the Russian software package CWB 4.3 [29] on the model of an isothermal plug-flow reactor. Table 2 shows the kinetic parameters of the considered heterogeneous processes for the three-parameter form of the Arrhenius equation:

$$k = AT^B \exp(-E/RT).$$

The values of particle accommodation coefficients on the reactor surface, γ_i, for the three heterogeneous reactions indicated in Table 2 were selected according to the procedure described in [26]: $\gamma(HO_2) = 2 \times 10^{-3}$, $\gamma(H_2O_2) = 1.1 \times 10^{-4}$, and $\gamma(CO) = 6.7 \times 10^{-8}$.

RESULTS AND DISCUSSION

The experimental temperature dependences of changes in the concentration of reagents and main products of propane oxycracking at the outlet of the reactor obtained in this study are shown in Figs. 1–3. The results of modeling based on various published mechanisms indicated in Table 1 are also presented there.

Figure 1a shows that almost all models give an underestimated value of the temperature of the onset of a rapid change in propane conversion at atmospheric pressure by about 25–50 K. The UBC and San Diego models describe this temperature dependence more accurately than the others; however, when describing the temperature dependence of oxygen conversion, the adequacy of these models is also low (Fig. 1b). The NG HIGH model is noticeably outside the general trend, which once again indicates the need to take into account the i-$C_4H_9O_2$ radicals and their subsequent low-temperature reactions when modeling such processes.

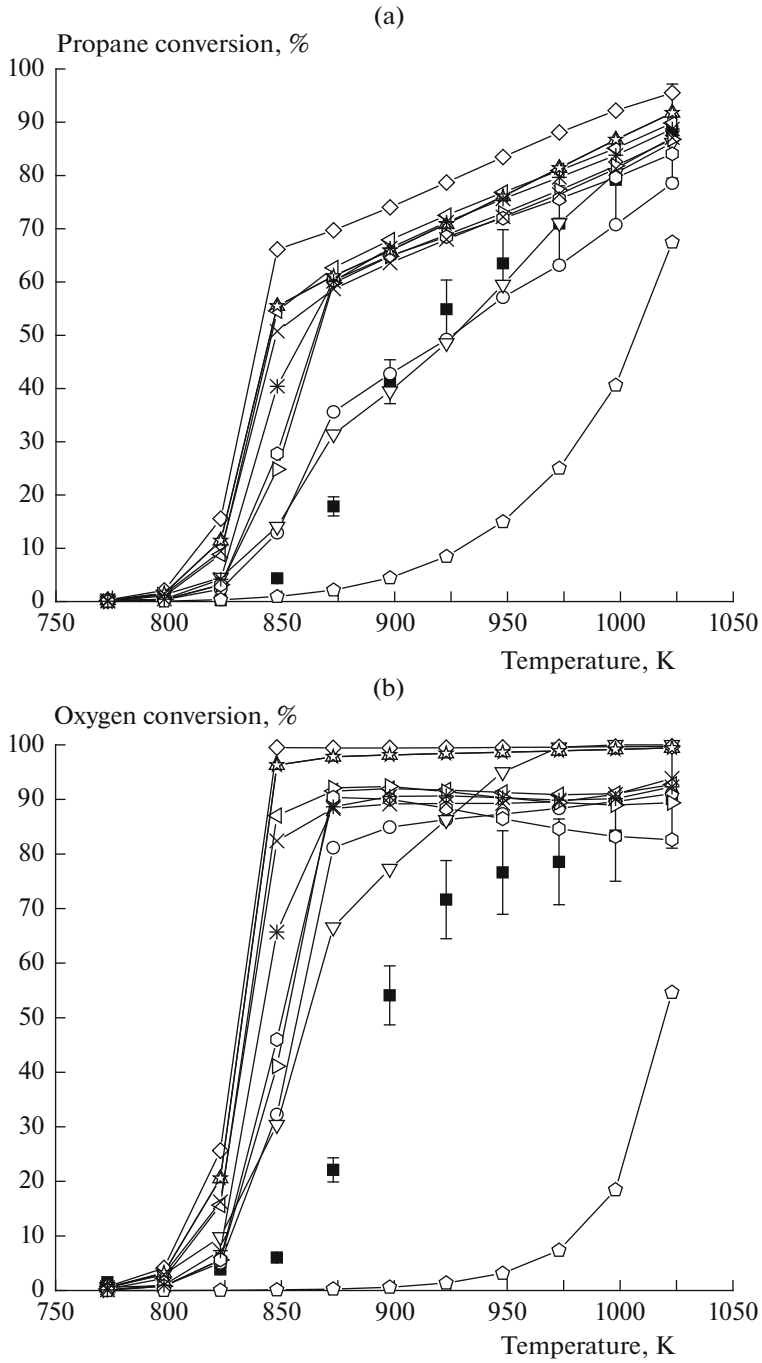

Fig. 1. Temperature dependence of propane (a) and oxygen (b) conversion at $P = 1$ atm, $[C_3H_8]_0 = 5.6\%$, $[O_2]_0 = 1.9\%$, diluent gas is nitrogen; ■, experimental values; –○–, San Diego; –△–, methane/propane; –▽–, UBC; –◇–, Ranzi; –◁–, Butan NUI; –▷–, Heptane NUI; –⬡–, Hexane NUI; –☆–, NG; –⬠–, NG High; –✕–, NG Low; –✳–, NG3.

One of the most important parameters for propane oxycracking is the maximum propylene concentration achievable. Almost all models show that the maximum propylene concentration is reached in the temperature range of 825 to 850 K (Fig. 2). In the case of the HEXANE NUI, HEPTANE NUI, NG LOW, and San Diego models, the temperature at which the concentration maximum is observed corresponds to ~873 K, which is ~50 K lower than the experimental value. The UBC, NG, and NG3 models also show an excessively low propylene concentration. The NG HIGH model again falls outside the general trend; hence, it was decided not to use it in the subsequent calculations.

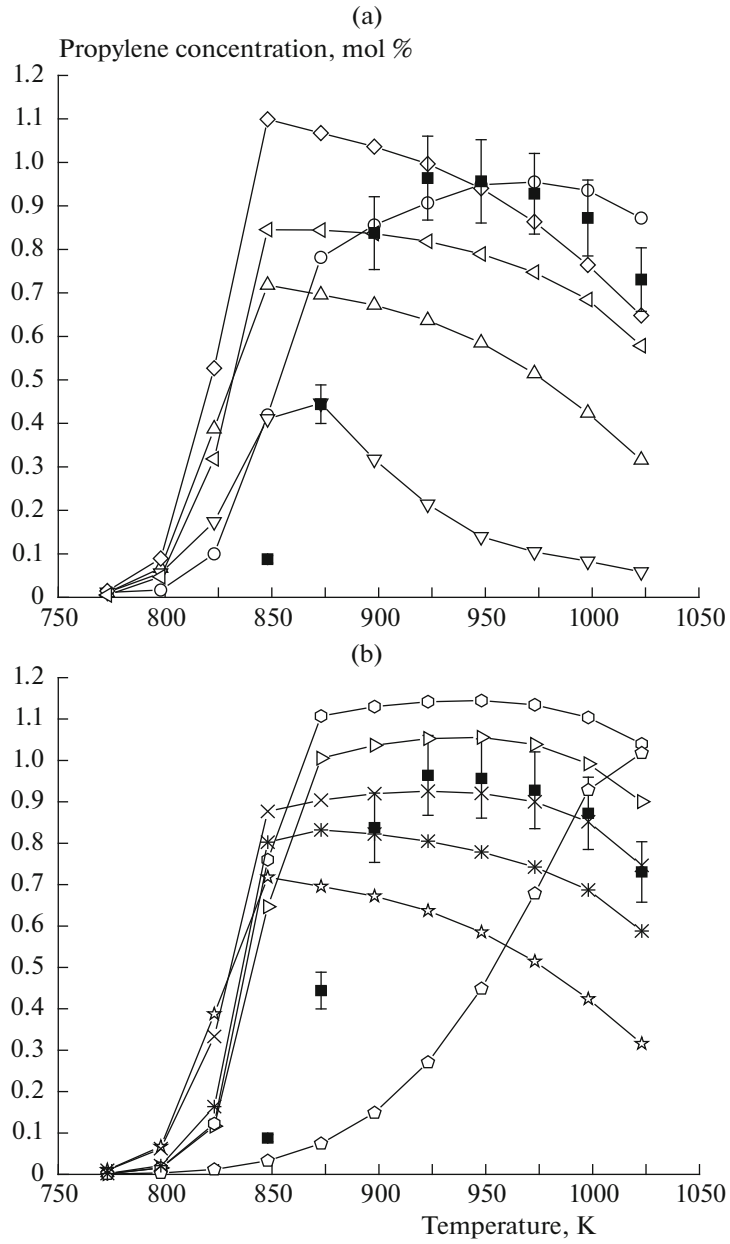

Fig. 2. Temperature dependence of the propylene concentration during the oxidative cracking of propane oxidative cracking of propane at $P = 1$ atm, $[C_3H_8]_0 = 5.6\%$; $[O_2]_0 = 1.9\%$, diluent gas is nitrogen. The designations are the same as in Fig. 1.

Propane oxycracking in methane, the main component of natural associated gas, is of great practical interest. Figure 3 shows the results of modeling this process using the models from Table 1. The calculations for all models give a lower reaction start temperature compared to the experimental values, as in [26], which confirms the need to take into account the processes on the reactor surface.

In accordance with the results obtained, the most adequate of the models we considered, NUIGMech, was supplemented by the three heterogeneous stages indicated in Table 2 with the parameters given there. Figure 4 shows a comparison of the experimental results with the results of NUIGMech propane oxycracking modeling with and without heterogeneous stages. The simulation results, taking into account the heterogeneous reactions quite well, actually quantitatively, describe the experimental results, which is a weighty argument in favor of the need to take into account heterogeneous reactions in laboratory-scale reactors.

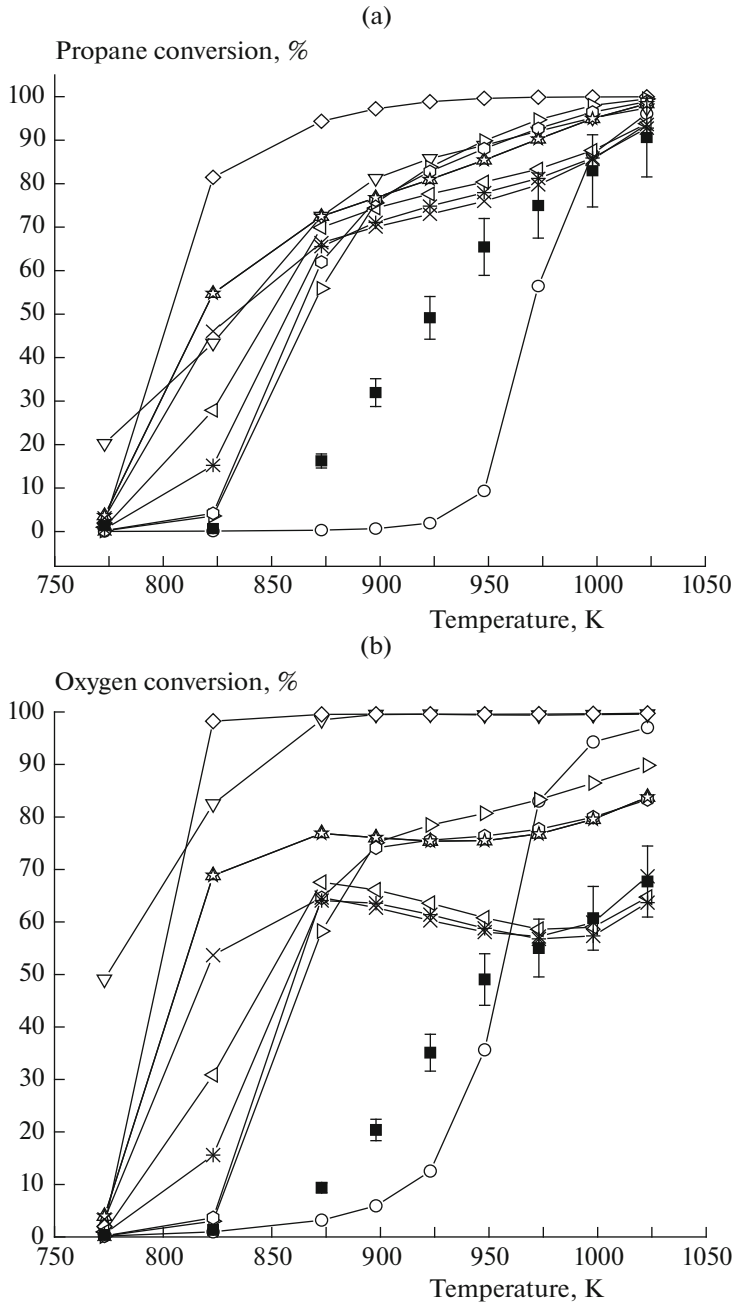

Fig. 3. Temperature dependence of propane (a) and oxygen (b) conversion in a methane environment at $[C_3H_8]_0 = 5.02\%$; $[O_2]_0 = 2.48$; $P = 1$ atm; diluent gas, methane. The designations are the same as in Fig. 1.

Similar results for another value of the initial propane/oxygen ratio are shown in Fig. 5. In this case, too, the results of modeling using the NUIGMech mechanism modified by adding heterogeneous steps are in quantitative agreement with the experimental results.

Thus, when the NUIGMech gas-phase mechanism is supplemented with reactions describing the most important heterogeneous processes on the reactor surface, the calculated temperature of the onset of a rapid increase in the conversion of reagents increases by ~50 K, which makes it possible to quantitatively reconcile the calculations with the experiments. Accounting for heterogeneous processes involving other radicals ($H^{\bullet}$, $OH^{\bullet}$, etc.), which play an important role in the gas-phase mechanism of oxycracking and ethane oxycracking [26] did not significantly affect the results, apparently due to the significantly higher rate of gas-phase processes with their participation.

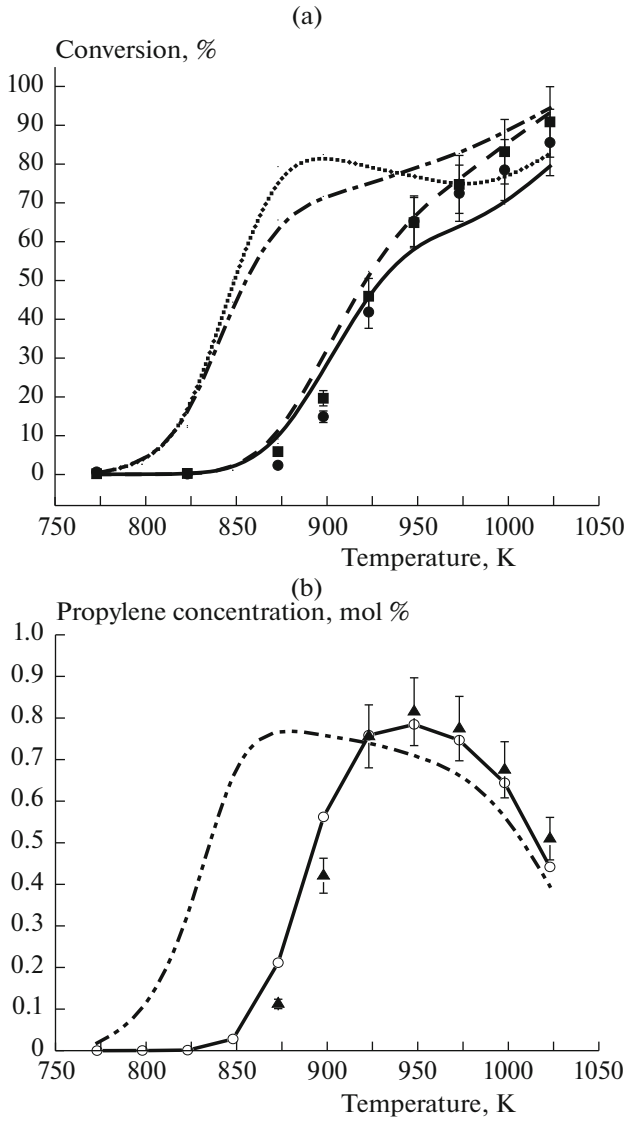

Fig. 4. Temperature dependence of propane (a) and oxygen (b) conversion and the maximum concentration of propylene (b) during propane oxycracking. Symbols, experimental results: ■, propane; ●, oxygen; ▲, propylene; the lines are the results of modeling according to the NUIGMech model without heterogeneous stages: the dashed-dotted curve is propane, the dotted line is oxygen, and the dashed line with two points is propylene; simulation results based on the NUIGMech model supplemented with heterogeneous stages: the dashed curve is propane, the solid curve is oxygen, —○— is propylen, $[C_3H_8]_0 = 4.59\%$ $[O_2]_0 = 2.49\%$, $P = 1$ atm, diluent gas is nitrogen.

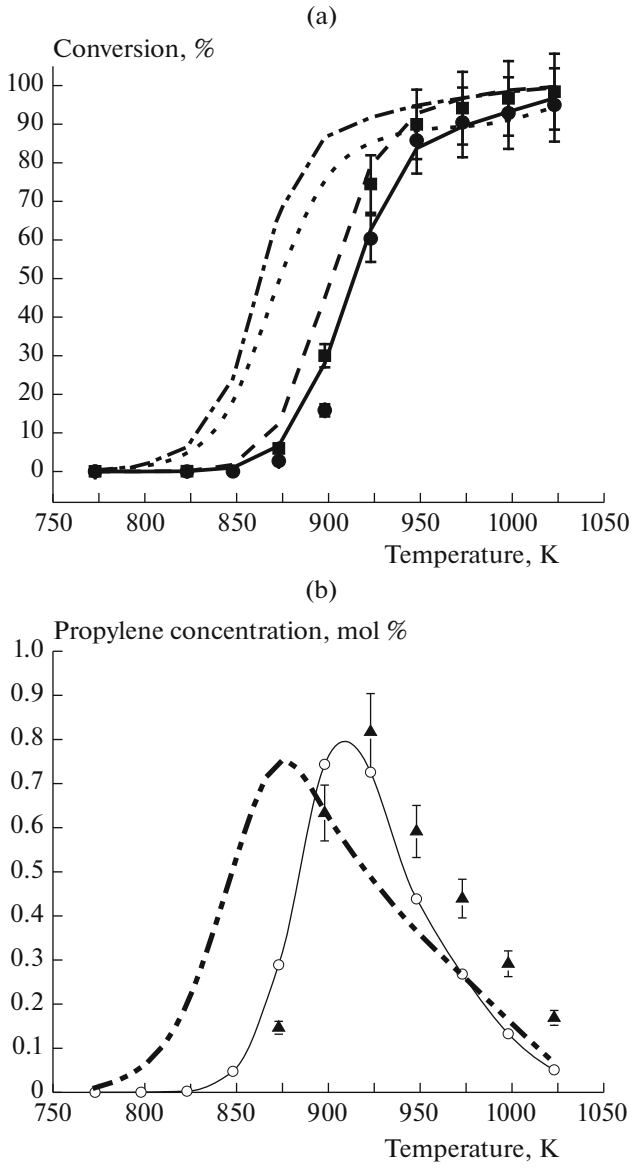

Fig. 5. The same as in Fig. 4, at $[C_3H_8]_0 = 4.65\%$ $[O_2]_0 = 5.05\%$.

CONCLUSIONS

Analysis of a large group of kinetic models of propane oxidation in the region of moderate temperatures ($T \leq 1000$ K) showed that the most modern models, such as NUIGMech, are able to qualitatively describe this process. However, a quantitative description of the process under the conditions of laboratory reactors with a high ratio of the area of the inner surface of the reactor to its volume requires taking into account the heterogeneous processes occurring on the surface of the reactor. Accounting for these processes with the kinetic parameters determined according to the technique proposed in [26, 28] makes it possible to obtain a quantitative, which is accurate up to the experimental error, agreement between the simulation results and experimental results.

FUNDING

The study was financially supported by the Russian Foundation for Basic Research and the Science Committee

of the Republic of Armenia as part of scientific project no. 20-53-05001.

REFERENCES

1. V. S. Arutyunov, R. N. Magomedov, A. Yu. Proshina, and L. N. Strekova, Chem. Eng. J. **238**, 9 (2014). https://doi.org/10.1016/j.cej.2013.10.009
2. V. S. Arutyunov, A. S. Dmitruk, and A. V. Nikitin, Russ. Chem. Bull. **65**, 2405 (2016). https://doi.org/10.1007/s11172-016-1597-3
3. R. N. Magomedov, A. Yu. Proshina, and V. S. Arutyunov, Kinet. Catal. **54**, 383 (2013). https://doi.org/10.1134/S0023158413040113
4. R. N. Magomedov, A. Yu. Proshina, B. V. Peshnev, and V. S. Arutyunov, Kinet. Catal. **54**, 394 (2013). https://doi.org/10.1134/S0023158413040125
5. A. S. Dmitruk, A. V. Nikitin, L. N. Strekova, and V. S. Arutyunov, in *Combustion and Explosion,* Ed. by S. M. Frolov (Torus Press, Moscow, 2016), Iss. 9, No. 3, p. 21.
6. J. Huang and W. K. Bushe, Combust. Flame **144**, 74 (2006). https://doi.org/10.1016/j.combustflame.2005.06.013
7. E. L. Petersen, D. M. Kalitan, S. Simmons, et al., Proc. Combust. Inst. **31**, 447 (2007). https://doi.org/10.1016/j.proci.2006.08.034
8. J. C. Prince, C. Treviño, and F. A. Williams, Combust. Flame **175**, 27 (2017). https://doi.org/10.1016/j.combustflame.2016.06.033
9. D. Healy, D. M. Kalitan, C. J. Aul, et al., Energy Fuels **24**, 1521 (2010). https://doi.org/10.1021/ef9011005
10. D. Healy, M. M. Kopp, N. L. Polley, et al., Energy Fuels **24**, 1617 (2010). https://doi.org/10.1021/ef901292j
11. N. Donato, C. Aul, E. Petersen, et al., J. Eng. Gas Turbine Power **132**, 051502 (2010). https://doi.org/10.1115/1.3204654
12. D. Healy, N. S. Donato, C. J. Aul, et al., Combust. Flame **157**, 1526 (2010). https://doi.org/10.1016/j.combustflame.2010.01.016
13. D. Healy, N. S. Donato, C. J. Aul, et al., Combust. Flame **157**, 1540 (2010). https://doi.org/10.1016/j.combustflame.2010.01.011
14. D. Healy, D. M. Kalitan, C. J. Aul, et al., Energy Fuels **24**, 1521 (2010). https://doi.org/10.1021/ef9011005
15. K. Zhang, C. Banyon, C. Togbé, et al., Combust. Flame **162**, 4194 (2015). https://doi.org/10.1016/j.combustflame.2015.08.001
16. K. Zhang, C. Banyon, J. Bugler, et al., Combust. Flame **172**, 116 (2016). https://doi.org/10.1016/j.combustflame.2016.06.028
17. G. Bourque, D. Healy, H. J. Curran, et al., Proc. ASME Turbo Expo. **3**, 1051 (2008). https://doi.org/10.1115/GT2008-51344
18. C1-C16 HT + LT + NOx mechanism, The CRECK Modeling Group, Politecnico di Milano. http://creckmodeling.chem.polimi.it/menu-kinetics/menu-kinetics-detailed-mechanisms/107-category-kinetic-mechanisms/406-mechanisms-1911-tot-ht-lt-nox/. Accessed 2020.
19. NUIGMech 1.1. https://c3.nuigalway.ie/combustionchemistrycentre/mechanismdownloads/
20. S. Martinez, M. Baigmohammadi, V. Patel, et al., Combust. Flame **228**, 401 (2021). https://doi.org/10.1016/j.combustflame.2021.02.009
21. Gri-Mech 3.0. http://combustion.berkeley.edu/gri_mech/version30/text30.html/
22. W. K. Metcalfe, S. M. Burke, S. S. Ahmed, and H. J. Curran, J. Chem. Kinet. **45**, 638 (2013). https://doi.org/10.1002/kin.20802
23. Y. Li, C. W. Zhou, K. P. Somers, et al., Proc. Combust. Inst. **36**, 403 (2016). https://doi.org/10.1016/j.proci.2016.05.052
24. C.-W. Zhou, Y. Li, E. O'Connor, et al., Combust. Flame **167**, 353 (2016). https://doi.org/10.1016/j.combustflame.2016.01.021
25. C.-W. Zhou, Y. Li, U. Burke, et al., Combust. Flame **197**, 423 (2018). https://doi.org/10.1016/j.combustflame.2018.08.006
26. M. G. Bryukov, A. S. Palankoeva, A. A. Belyaev, and V. S. Arutyunov, Kinet. Catal. **62**, 703 (2021). https://doi.org/10.1134/S0023158421060021
27. J. A. Miller and S. J. Klippenstein, Int. J. Chem. Kinet. **33**, 654 (2001). https://doi.org/10.1002/kin.1063
28. A. S. Palankoeva, Ya. S. Zimin, M. G. Bryukov, A. A. Belyaev, and V. S. Arutyunov, Gorenie Vzryv **14** (4), 42 (2021). https://doi.org/10.30826/CE
29. Chemical Workbench 4.3. Kintech Laboratory. http://www.kintechlab.com/products/chemical-workbench/. Accessed 2021.